PHYSICAL REVIEW B VOLUME 19, NUMBER 3 1 FEBRUARY 1979

Microscopic critical dynamics of one-dimensional spin systems*

George Reiter
Instituto de Ciencas Exatas, Universidade Federal de Minas Gerais, Brazil, Physics Department, Texas A&M University, College Station, Texas 77843, and Ames Laboratory, Ames, Iowa 50011
(Received 17 March 1978)

We present an exact solution for the spin-spin correlation function of the dynamical spherical model (the spherical-model equilibrium state together with the classical-Heisenberg-model equations of motion) in one dimension at $T = 0$. The physical picture of the system is clarified, as is the difference between the Heisenberg and dynamical spherical model arising from the presence of the constraint $\vec{S}_i \cdot \vec{S}_i = 1$ in the former model. The effect of the higher-order correlations, induced by the constraint, on the dynamics is made explicit. The solution satisfies the dynamical-scaling hypothesis. The mode-coupling approximation, although it gives the correct dynamical exponents, yields a qualitatively incorrect spectral function. It cannot be improved by including higher-order terms in the expansion of the self energy in terms of the number of interactions (the extended-mode-coupling theory), as the higher-order terms yield physically unrealistic solutions. A qualitatively correct approximate solution has been found, that exhibits both the central peak and the spin wave sidebands of the exact solution. The solution cannot be improved by including higher-order terms either. There does not appear to be any way of constructing a series of approximations from the leading terms in a renormalized-perturbation-series expansion that will converge to the exact solution.

The classical Heisenberg Hamiltonian has the remarkable property that there are two qualitatively different stationary states of the system at any temperature. These differ in that in one case, the constraint

$$\frac{1}{N}\sum \langle \vec{S}_i \cdot \vec{S}_i \rangle = 1$$

is imposed, and the stationary state is described by the dynamical spherical model, and in the other case, the constraint $\vec{S}_i \cdot \vec{S}_i = 1$ leads to the Heisenberg model. In four dimensions or more, the static critical behavior of both models is identical, and so we would expect the critical dynamics to be, although this has not been proven. Below four dimensions, the spherical-model fixed point becomes unstable for ϕ^4 models, which are believed to be adequate approximations to the Heisenberg model for calculating static properties, if the dimension is greater than 2. The dynamical spherical model is interesting in its own right, however, even if it does not describe the same critical dynamics as the Heisenberg model. It combines the simplest static critical behavior with the simplest nonlinear dynamics, and it is the only existing model for which the mode-coupling theory and its extension to higher numbers of interacting modes is known to provide the correct formal solution for the spectral functions.[1,2] One can show, term by term in the expansion in the number of interacting modes, that the dynamical scaling hypothesis is valid, although the convergence properties of this expansion are unknown, and will be part of the subject of this paper.

We wish to discuss the relationship between the two models in one dimension, where $T = 0$ plays the role of a critical temperature. Our original interest in this comparison was to understand more of the mechanism for the appearance of "sloppy spin waves," that is, spin waves in the absence of an ordered phase. The Heisenberg model at $T = 0$ has a spin-fluctuation spectrum describable by perfectly-well-defined spin waves, whereas, as we will show, the spherical model does not, despite the fact that both show diverging coherence lengths, with the same critical exponent. The spectral function for the spherical model at $T = 0$ has not been known previously, and we present the exact solution. The comparison gives a clear understanding of the role of the constraint in the dynamics, and a clear physical picture of these systems at $T = 0$. We will discuss also the role that the range of the interaction plays in the dynamics. The spherical model is known to be the infinite-interaction-range limit of the Heisenberg model. We conclude that there is a dynamical crossover phenomenon in which well-defined spin waves exist for any arbitrary but finite-range interaction. The exact solution for the spherical model at $T = 0$ also elucidates the nature of the mode-coupling approximation, in particular the kind of errors one makes by keeping only the lowest-order term in an expansion in the number of vertices. We find that the expansion is not

 ©1979 The American Physical Society

"well behaved," in the sense that nonphysical results are obtained in higher orders.

Section I is for the most part a review of salient facts about the dynamical spherical model, and is intended to serve as an introduction. Section II is the derivation of the exact solution for the spherical model at $T=0$. Section III is a comparison with the Heisenberg model and a discussion of the effect of the interaction range, Section IV discusses various mode-coupling approximations and the kinetic theory developed for the dynamical spherical model.[3]

I. INTRODUCTION

The classical Heisenberg Hamiltonian

$$H=-\frac{1}{2}\sum_{i,j}J_{ij}\vec{S}_i\cdot\vec{S}_j \tag{1}$$

and the usual spin commutation relations, interpreted as Poisson brackets here, lead to the equation of motion

$$\frac{\partial S_i^\alpha}{\partial t}=\sum J_{ij}\epsilon^{\alpha\beta\gamma}S_i^\beta S_j^\gamma\,, \tag{2}$$

where $\epsilon^{\alpha\beta\gamma}$ is the antisymmetric tensor of rank 3. It follows immediately that

$$\frac{\partial}{\partial t}\vec{S}_i\cdot\vec{S}_i=2\sum J_{ij}S_i^\alpha S_i^\beta S_j^\gamma\epsilon^{\alpha\beta\gamma}=0\,. \tag{3}$$

And hence we are free to fix the length of the spin on each site independently.

If we make the choice that $\vec{S}_i\cdot\vec{S}_i=1$, we obtain the Heisenberg model, and the phase space may be restricted to the tensor product of unit spheres for each site. Since we wish to consider a more general situation, we will take as the phase space R^{3N}, where N is the number of sites. We will call the "Heisenberg state" the distribution in the phase space with support on the tensor product of unit spheres defined by

$$\rho_H(\vec{S}_1,\ldots,\vec{S}_N)=e^{-\beta H(\vec{S}_1,\ldots,\vec{S}_N)}. \tag{4}$$

For the spherical model, S_i^α are Gaussian random variables, for which $N^{-1}\sum_i\langle\vec{S}_i\cdot\vec{S}_i\rangle=1$. The spherical-model state is given by the distribution

$$\rho_S(\vec{S}_1,\ldots,\vec{S}_N)=\exp\left[-\beta\left(H-\mu\sum_i\vec{S}_i^2\right)\right], \tag{5}$$

where μ is chosen as function of β so that the constraint $N^{-1}\sum_i\langle\vec{S}_i\cdot\vec{S}_i\rangle=1$ holds. It is also possible to fix arbitrarily the magnitude of the spin on each site, and obtain a stationary state (without translation invariance), or to allow the spin length at each site to have some other distribution other than that given by (5). This may actually be a useful model for the description of some impurity problems.

It is rather remarkable that (5) is indeed a stationary state of the dynamics given by (2). This is by no means obvious.

The proof that this distribution is stationary has been given by Van Leeuwen and Gunton,[2] and in a slightly different context, by the author.[1] A straightforward proof of this fact can be obtained by showing that

$$\frac{\partial}{\partial t}\langle S_{i_1}^{\alpha_1}\cdots S_{i_n}^{\alpha_n}\rangle\Big|_{t=0}=0 \tag{6}$$

for all α, when (2) is used to compute the time derivatives and (5) to calculate the average $\langle\ \rangle$. This is demonstrated in Appendix A. Since the spherical-model state is stationary, we can calculate equilibrium response functions, and in particular, we shall be interested in $\Sigma_q(t)=\langle S_q^0(t)S_{-q}^0\rangle$.

It is convenient to introduce a Hilbert-space structure for this purpose. Consider the linear vector space of all functions of the spin variables associated with each site, which we will call V. For our purposes, this has as basis all function of the form $S_{q_1}^{\alpha_1},\ldots,S_{q_n}^{\alpha_n}$, n arbitrary. Then for any two elements A and B in V, we can define an inner product as

$$\langle A|B\rangle=\langle A^\dagger B\rangle\,, \tag{7}$$

which allows us to regard the random variables $S_{q_1}^{\alpha_1}\cdots S_{q_r}^{\alpha_r}$ elements of V, as states in the Hilbert space. Physically, these states correspond to the superposition of n fluctuations on the equilibrium background defined by the spherical model. We define the Liouville operator L, which is an operator on V, to be the generator of the dynamical group, i.e., $A(t)=e^{-tLt}A$. The action of L on any element of V is explicity

$$L[A]=-i\{H,A\}\,, \tag{8}$$

where $\{\ ,\ \}$ is a Poisson bracket, and may be determined from the basic relations (2).

The Laplace transform of $\Sigma_q(t)$ is

$$\Sigma_q(z)=\int_0^\infty e^{izt}\langle S_q^0|\,S_q^0(t)\rangle\,dt=i\langle S_q^0|(z-L)^{-1}|S_q^0\rangle \tag{9}$$

and is the diagonal matrix element of the resolvent of the Liouville operator. It can be shown that L is an Hermitian operator. This follows readily from the stationarity of ρ_S.

We shall calculate $\Sigma_q(z)$ by summing the terms in the moment expansion

$$\Sigma_q(z)=\frac{i\langle S_q^0|S_q^0\rangle}{z}\sum_{r=0}^{\infty}\frac{\omega_q^{2n}}{z^{2n}}\,, \tag{10}$$

where

$$\omega_q^{2n}=\langle S_q^0|L^{2n}|S_q^0\rangle/\langle S_q^0|S_q^0\rangle\,.$$

This expansion is convergent in the time domain. If we introduce normalized spin amplitudes $\tilde{S}^{\alpha} = S_q^{\alpha}/\langle S_q^{\alpha}|S_q^{\alpha}\rangle^{1/2}$, we can imagine writing a resolution of the identify on V is

$$I = |1\rangle\langle 1| + \sum_{q,\alpha} |\tilde{S}_q^{\alpha}\rangle\langle\tilde{S}_q^{\alpha}| + \frac{1}{2!}\sum_{q_1 q_2} |\tilde{S}_{q_1}^{\alpha_1}\tilde{S}_{q_2}^{\alpha_2}\rangle\langle\tilde{S}_{q_1}^{\alpha_1}\tilde{S}_{q_2}^{\alpha_2}| + \cdots, \tag{11}$$

where $|1\rangle$ is the spherical-model state. Equation (11) is actually not correct, as the states in the expansion are not orthogonal. Nevertheless, the result obtained by inserting (11) between powers of L in the matrix element that defines the moments is correct, the corrections due to nonorthogonality canceling.[1] That is,

$$\omega_q^{2n} = \sum_{\substack{\text{all intermediate}\\ \text{states}}} \langle\tilde{S}_q^0|L|\tilde{S}_{q_1}^{\alpha_1}\cdots\tilde{S}_{q_n}^{\alpha_n}\rangle\langle\tilde{S}_{q_1}^{\alpha_1}\cdots\tilde{S}_{q_n}^{\alpha_n}|L|\tilde{S}_{q_{i_1}}^{\alpha_{i_1}}\cdots\tilde{S}_{q_{i_m}}^{\alpha_{i_m}}\rangle\cdots\langle\tilde{S}_{q_{i_1}}^{\alpha_{i_1}}\cdots\tilde{S}_{q_{i_p}}^{\alpha_{i_p}}|L|\tilde{S}_q^0\rangle \tag{12}$$

The moments can, in this way, be represented as sum of products of matrix elements of L, and it is convenient to represent these matrix elements graphically. A state can be represented by a number of horizontal lines, one for each factor of $S_{q_i}^{\alpha}$ appearing labeled with q, α. The index can be coded in the representation of the line, as in Ref. 1, but for our purpose, it is preferable to treat the spin index on the same footing as the wave vector, and whereas it is usually most convenient to use spherical tensors for the basis, i.e., $\alpha_i = \pm 1, 0$ we will use Cartesian components. The general matrix element is shown in Fig. 1. There is only one basic vertex, corresponding to the matrix element $\langle\tilde{S}_{q_1}^{\alpha_1}|L|\tilde{S}_{q_2}^{\alpha_2}\tilde{S}_{q_3}^{\alpha_3}\rangle$ and its adjoint and this has the value

$$i\delta(q_1+q_2+q_3)(J_{q_2}-J_{q_3})\rho_{q_2}^{1/2}\rho_{q_3}^{1/2}\rho_{q_1}^{-1/2}\epsilon^{\alpha_1\alpha_2\alpha_3}, \tag{13}$$

where

$$\rho_q \equiv \langle S_q^{\alpha}|S_q^{\alpha}\rangle. \tag{14}$$

The $2n$th moment is obtained by forming all possible diagrams containing n right and n left vertices, and summing over the internal spin indices and wave-vector coordinates. For instance, the second and fourth moment diagrams are shown in Fig. 2.

The analytic expression for the second moment is

$$\omega_q^2 = \frac{1}{2}\sum_{q_2 q_3} \delta(q+q_2+q_3)(J_{q_2}-J_{q_3})^2(\epsilon^{\alpha\alpha_2\alpha_3})^2\rho_{q_2}\rho_{q_3}\rho_q^{-1}. \tag{15}$$

The analytic expression for the fourth moment is given in Ref. 2.

An expansion analogous to (11) was used by Kadanoff and Swift[4] to obtain the mode-coupling theory for the liquid-gas transition. In that context, there is no reason to suspect that the results obtained are the exact expression of the microscopic dynamics. Here, however, the mode-coupling theory and its generalization to higher number of interactions, which we will call the extended-mode-coupling theory, is a representation of the exact microscopic dynamics, and can be obtained by summing diagrams in the moment expansion.[1] (See Appendix B and the review article by Kawasaki.[5]) We sketch the derivation.

The diagrams for the moments may be regarded as contributions to the expansion (10) if we associate a factor of z^{-1} with each vertex. Then, defining a self-energy $\tilde{\phi}_q(z)$ to be the sum of all diagrams that contain no single internal line [excluding diagram 2(b) for instance], we have

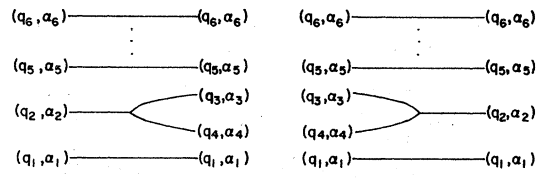

FIG. 1. Most-general matrix elements of L.

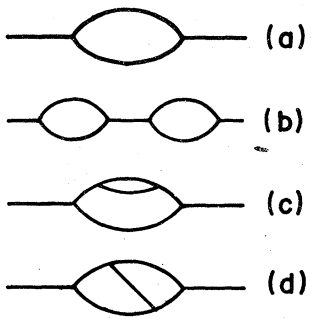

FIG. 2. Diagrams for the second (a) and fourth moments (b)–(d).

$$\Sigma_q(z) = i\langle S_q^0 | S_q^0\rangle z^{-1}[1 + \tilde{\phi}_q(z) + \tilde{\phi}_q(z)^2 + \cdots]$$
$$= i\langle S_q^0 | S_{-q}^0\rangle [z - \phi_q(z)]^{-1}; \quad (16)$$

$\phi_q(z) = z\tilde{\phi}_q(z)$. $\tilde{\phi}_q(z)$ is given diagrammatically in Fig. 3, the crosshatching indicating all possible diagrams that do not have a single line as an intermediate state.

Every distinct sequence of intermediate states corresponds to a distinct diagram. Diagrams with the same topological structure that differ only in the sequence from left to right that vertices occur, such as shown in Fig. 4, have the same value, and may be readily summed. In the present context, a simple way of obtaining the result was given by Wegner.[6] If we label each internal vertex with a time t_i, $i = 1, \ldots, n$, beginning on the left, the total contribution from all diagrams with the same topological structure is

$$(-i)^{n+1}\int_0^t \cdots \int_0^t dt_1 \cdots dt_n \prod \Theta(t_{i_1} - t_{i_2}) A_n ,$$

where A_n is the value of a single diagram of the particular structure, and there is a factor of $\Theta(t_{i_1} - t_{i_2})$ for each line joining a vertex at t_{i_1} with another at t_{i_2} [$\Theta(t) = 1$, $t \geq 0$, $\Theta(t) = 0$, $t < 0$]. If we take any line between two vertices and replace it by the full propagator $\Sigma_q(t)/\Sigma_q(0)\Theta(t)$, which we will call $G_q(t)$ we sum all those diagrams obtained by putting all possible insertions (that is, self-energy subdiagrams) on that line, whatever the rest of the diagram is. All of the diagrams may therefore be obtained by summing over all skeleton diagrams, that is moment diagrams that have no insertions, and replacing the lines by the full propagator $G_q(t)$. $\Theta_q(t)$ is then the sum over all skeleton diagrams with this replacement. If we denote the contribution from diagrams with n vertices as $\phi_q^n(t)$, the lowest-order term is

$$\phi_q^2(t) = -i\Theta(t)\sum_{q_1 q_2} \delta(q + q_1 + q_2)(J_{q_1} - J_{q_2})^2 \times G_{q_1}(t) G_{q_2}(t) \rho_{q_1}\rho_{q_2}\rho_q^{-1}. \quad (17)$$

This is the mode-coupling result, and corresponds to diagram 2(a), with the lines replaced by the appropriate propagators. The next term, $\phi_q^4(t)$, is obtained from diagram 2(d), with the same replacements. Expression (15) may also be obtained using projection operators. $\phi_q(t)$ can be shown to be

FIG. 3. Self-energy for the spin fluctuations.

FIG. 4. Equivalent diagrams differing only in the time ordering of the vertices.

$$\phi_q(t) = -i\sum_{q_1 q_2 q_3 q_3} \delta(q + q_1 + q_2)\delta(-q + q_3 + q_4) \times (J_{q_1} - J_{q_2})(J_{q_3} - J_{q_4}) \times \langle S_{q_1}^{-1}(t) S_{q_2}^{+1}(t) S_{q_3}^{-1} S_{q_4}^{+1}\rangle \rho_q^{-1} , \quad (18)$$

where the time dependence in (18) is modified, the modification being equivalent to omitting intermediate states with single lines in the diagrams. The independent-mode approximation corresponds to the factorization

$$\langle S_{q_1}^{\alpha}(t) S_{q_2}^{\beta}(t) S_{q_3}^{-\alpha} S_{q_4}^{-\beta}\rangle = \delta_{q_1+q_3}\delta_{q_2+q_4}\langle S_{q_1}(t) S_{-q_1}^{-\alpha}\rangle\langle S_{q_2}^{\beta}(t) S_{-q_2}^{-\beta}\rangle \quad (19)$$

and leads immediately to Eq. (17). The mode-coupling equation for the spin system was first obtained in this way by Kawasaki.[7] A similar equation, valid for long-range interactions, had been obtained earlier by Resibois and De Leneer,[8] using diagrammatic methods applicable to spin $\frac{1}{2}$. The equation was obtained later by Wegner,[6] using diagrammatic techniques similar to those described here, and by Blume and Hubbard[9] by other methods.

The independent-mode approximation is correct at $t = 0$ for the dynamical spherical model [see Eq. (A4)]. The higher-order terms with $\phi_q^n(t)$, $n > 2$, give the buildup of correlations between the modes as they propagate. For times such that $tJS \gg 1$, there is no reason to suspect that the higher-order terms are not significant, other than the intuitive sense that very complex correlations have little effect on the dynamics of a single mode.

In the Heisenberg model, this approximation is not even correct at $t = 0$, due to the presence of higher-order correlations in the Heisenberg state, induced by the constraint $\vec{S}_i \cdot \vec{S}_i = 1$.[10] One way of treating these correlations is to admit additional vertices. For instance,

$$\langle S_{q_1}^{\alpha_1} S_{q_2}^{\alpha_2} | L | S_{q_3}^{\alpha_3} S_{q_4}^{\alpha_4} S_{q_5}^{\alpha_5}\rangle \neq 0$$

in the case that there does not exist a set of indices, say, $q_1\alpha_1$ and $q_3\alpha_3$, such that $\alpha_1 + \alpha_3 = 0$, $q_1 + q_3 = 0$. This matrix element of L cannot be represented in terms of $\langle S_{q_1}^{\alpha_1} | L | S_{q_4}^{\alpha_4} S_{q_5}^{\alpha_5}\rangle$ and $\langle S_{q_3}^{\alpha_3} S_{q_2}^{\alpha_2}\rangle$. That is, a diagram such as 5(a) must be supplemented by a diagram such as 5(b), that contains the correction due to nonvanishing four-spin cumulant averages. These correlations have a profound effect on the dynamics, in one dimension. In fact, the sum of the diagrams shown in Fig. 6, which is

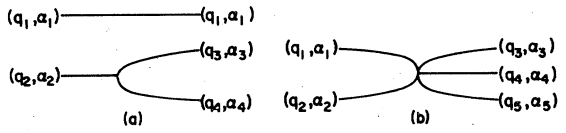

FIG. 5. Contribution to the matrix element

$$\langle S^{\alpha_1}_{q_1} S^{\alpha_2}_{q_2} \mid L \mid S^{\alpha_3}_{q_3} S^{\alpha_4}_{q_4} S^{\alpha_5}_{q_5} \rangle$$

arising from pair correlations (a) and from nonvanishing four-spin cumulants (b).

equal to $\omega_q^4 - (\omega_q^2)^2$, vanishes linearly with KT in the Heisenberg model, although any term separately is proportional to $(\omega_q^2)^2$. The higher-order correlations, and the dynamical processes they induce, are thus directly responsible for the appearance of well-defined spin-wave modes [the vanishing of $\omega_q^4 - (\omega_q^2)^2$ implies that the spin-wave modes are perfectly well defined].

We note that the formally exact perturbation theory developed by Martin, Siggia, and Rose[11] would probably be incapable of treating the Heisenberg chain since the correlations induced by the constraint appear only in the vertex corrections, and presumably these would have to be retained to all orders in order to get the correct equilibrium four-spin correlations, which would be required to obtain the cancellation just mentioned. As we shall see in Sec. IV, even for the spherical model, where there are no additional vertices, the perturbation solution is not well behaved.

It has been shown by Van Leeuwen and Gunton[2] and earlier, in unpublished work, by Riedel and Wegner,[12] that the assumption that

$$\lim_{k\to 0} \Sigma_q(\omega,\kappa)/\langle S_q^0/S_q^0\rangle \to \kappa^{-z}\,\Sigma^*_{\rho_1}(\rho_2)\,, \tag{20}$$

where $\rho_1 = q/\kappa$, $\rho_2 = \omega/\kappa^z$ was consistent term by term in the extended-mode-coupling expansion. That is, if (26) was assumed, then for all n

$$\lim_{k\to 0} \phi_q^{2n}(\omega,\kappa) \to \kappa^z \phi^{*2n}_{\rho_1}(\rho_2)\,,$$

κ is the inverse coherence length. These proofs have been given for $T_c > 0$, but are essentially unmodified in the present case of one dimension. The primary difference is in the exponent z, which does not extrapolate from the values in higher dimension and in particular is not equal to $\frac{1}{2}d$ in the antiferromagnet.

Although no proof has been given that $\sum_n \phi^{2n}_{\rho_1}(\rho_2)$ exists, that is, that we can exchange the summation and limiting process, we shall see that at $T=0$, for fixed q and ω, (20) is satisfied. If we assume it is the case for arbitrary ρ_1, ρ_2, then the dynamical spherical model satisfies the dynamical scaling hypothesis. We take the statement of the dynamical scaling hypothesis to be that (20) holds with arbitrary ρ_1, ρ_2.

We conclude this section by pointing out that these results can be extended to the anisotropic dynamical spherical model, with the Hamiltonian

$$H = -\sum J_{ij}\,\vec{S}_i \cdot \vec{S}_j - \sum A_{ij} S_i^0 S_j^0\,,$$

as has been demonstrated by Barreto and the author.[13]

II. EXACT SOLUTION AT $T=0$

Although it is generally impossible to sum all the diagrams in the moment expansion, this can be accomplished in one dimension at $T=0$. In this case

$$\rho_q \to \tfrac{1}{3}\delta(q - q_c)\,, \tag{21}$$

where $q_c = 0$ (ferromagnet) or π/a (antiferromagnet). As a consequence, the summation over the wave-vector indices becomes trivial. We will treat first the ferromagnet. Consider a segment of the diagram that begins as shown in Fig. 7. Although we have given a symmetric definition of the right and left vertices, involving $\rho_q^{1/2}$, the structure of the diagrams is such that we can associate a factor of $\rho_{q_1}\rho_{q_2}/\rho_q$ with either the right (left) vertices, and a factor of unity with the left (right) vertices. We choose the temperature renormalization factor to be associated with the left vertices. Then the wave-vector sum reduces to two terms $q_1 = 0$, $q_2 = q$ and $q_1 = q$, $q_2 = 0$. The value of the first vertex is $i(J_0 - J_q)\epsilon^{\nu_1\nu_0\nu_q}$ in both cases. ν_1 is the incoming index, ν_0 the index of the line with $q=0$. If $q_2 = 0$, the entire diagram is zero since the second vertex vanishes ($q_3 = -q_4$).

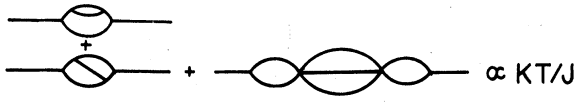

FIG. 6. Diagrammatic contributions to $\omega_q^4 - (\omega_q^2)^2$ for the Heisenberg model. The diagram due to the nonvanishing four-spin cumulants, present because of the constraint $\vec{S}_i \cdot \vec{S}_i = 1$, cancels the remaining diagrams at $T=0$.

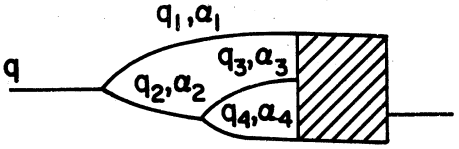

FIG. 7. Structure of the self-energy for arbitrary temperatures.

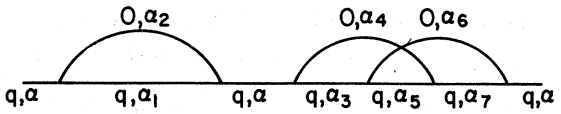

FIG. 8. Typical diagram that is nonvanishing at $T=0$, for the ferromagnet.

Nonvanishing contributions can be obtained only when the line whose wave-vector index is zero is connected directly to an incoming line of a right vertex. This is true of the second and all subsequent left vertices as well. The general structure of the diagrams must then be as shown in the example of Fig. 8. The right vertices are equal to $i(J_0-J_q)\epsilon^{\nu_i\nu_0\nu_f}$ if we adopt the convention that ν_i is the index associated with the line of wave vector q incoming from the left, and ν_f that of the line leaving on the right. That is, they have the same value as the left vertices. All the nonvanishing diagrams can be generated by the following rules for a diagram of order $2n$. (i) Beginning and ending with a particular spin index, label $2n$ vertices of the sort shown in the example of Fig. 9 with a consistent set of spin indices. That is, all three spin indices must be different. (ii) Associate with each vertex a factor of $i(J_0-J_q)\epsilon^{\nu_i\nu_0\nu_f}$. (iii) Multiply by $(\frac{1}{3})^n$. (iv) Pair all vertical lines with the same spin index in all possible ways. (v) Sum over all possible consistent spin indices. The $2n$th moment is the sum of all such contributions. In order to calculate this sum, we will consider an equivalent problem, that may be transformed into a readily solvable one.

We construct a model, which we will call the averaged spherical model, for which all the random variables S_q in an interval $-\epsilon<q<\epsilon$ are replaced by a single mode S_0^α, where

$$S_0^\alpha=\int_{-\epsilon}^{\epsilon} S_q^\alpha\,dq\,. \tag{22}$$

Modes outside of this interval are distributed according to the spherical-model distribution (5). S_0^α is the sum of Gaussian random variables, and is itself a Gaussian random variable, with

$$\langle(S_0^\alpha)^2\rangle=\int_{-\epsilon}^{\epsilon}\langle S_q^\alpha S_{-q}^\alpha\rangle\,dq\,. \tag{23}$$

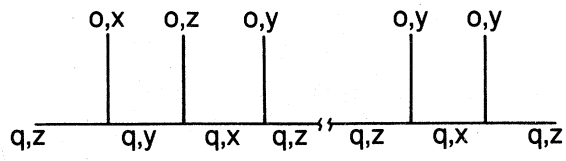

FIG. 9. Most-general vertex before pairing equivalent spin indices, for the ferromagnet.

As $T\to 0$, $\langle(S_0^\alpha)^2\rangle\to\frac{1}{3}$, for any ϵ. Evidently, for T sufficiently small, we may take ϵ as small as we please and still have $\langle(S_0^\alpha)^2\rangle=\frac{1}{3}-\delta$ with δ arbitrarily small. The distribution function for the averaged spherical model has a limit as $T\to 0$, for which $\langle(S_0^\alpha)^2\rangle=\frac{1}{3}$ and $\langle S_q^\alpha S_{-q}^\alpha\rangle=0$, whereas the spherical model does not. Furthermore, for the limiting distribution we can take $\epsilon\to 0$, and the distribution remains well defined. Let us consider calculating for this model,

$$R_q(t)\equiv\lim_{\epsilon\to 0}\lim_{T\to 0}\langle S_q^\alpha(t)S_{-q}^\alpha(0)\rangle/\langle S_q^\alpha S_{-q}^\alpha\rangle \tag{24}$$

with $q>0$ fixed. The average can be done in two steps. We can first calculate

$$R_{S_0}(q,t)=\langle S_q^\alpha(t,\vec{S}_0)S_{-q}^\alpha(0,\vec{S}_0)\rangle_{\vec{S}_0}/\langle S_q^\alpha S_{-q}^\alpha\rangle_{S_0} \tag{25}$$

where $\langle\ \rangle_{\vec{S}_0}$ is the average over the conditional distribution of the $\vec{S}_q$, given the value of $\vec{S}_0$ at $t=0$. $\vec{S}_q(t,\vec{S}_0)$ is the time evolution of $\vec{S}_q(t)$ given the initial value of $\vec{S}_0$. We can then calculate

$$\langle S_q^\alpha(t)S_{-q}^\alpha(0)\rangle=\int P(\vec{S}_0)R_{\vec{S}_0}(q,t)\,d\vec{S}_0\,. \tag{26}$$

Since $\vec{S}_0$ and $\vec{S}_q$ are independently distributed

$$\langle S_q^\alpha S_{-q}^\alpha\rangle=\langle S_q^\alpha(0,\vec{S}_0)S_{-q}^\alpha(0,\vec{S}_0)\rangle_{\vec{S}_0}=\rho_q\,. \tag{27}$$

The time dependence of the modes is determined by the equations of motion (7). For $\vec{S}_0$ we have

$$\frac{\partial\vec{S}_0}{\partial t}=O(\epsilon)\,. \tag{28}$$

Hence, for any fixed q and t, (25) may be calculated by assuming that S_0 is a constant. Near $T=0$ the amplitude of the fluctuations $\vec{S}_q$ will be much smaller than $\vec{S}_0$, with a probability that approaches 1. Consequently, we can evaluate the time evolution of $S_q(t,S_0)$ from the usual linearized spin-wave equations of motion. That is,

$$i\frac{\partial S_q^\alpha(t,\vec{S}_0)}{\partial t}=i(J_0-J_q)\epsilon^{\alpha\beta\nu}S_0^\beta S_q^\nu(t,\vec{S}_0)\,. \tag{29}$$

The $2n$th moment of (24) is therefore

$$\langle\omega^{2n}\rangle_q=\int\frac{\langle[(i\,\partial/\partial t)^{2n}S_q^\alpha(t,\vec{S}_0)]S_{-q}^\alpha(0,\vec{S}_0)\rangle_{t=0}P(\vec{S}_0)\,d\vec{S}_0}{\langle S_q^\alpha S_q^\alpha\rangle}\,. \tag{30}$$

Using (29) and the fact that S_q^α and $\vec{S}_0$ are independently distributed, together with (27) we have

$$\langle\omega^{2n}\rangle_q=[i(J_0-J_q)]^{2n}\epsilon^{ij}\cdots\epsilon^{k_{2n-1}j_{2n}}\langle S_0^{j_1}\cdots S_0^{j_{2n}}\rangle\,. \tag{31}$$

This is identical to the moments of the dynamical spherical model, at $T=0$, since $\langle S_0^{j_1}\cdots S_0^{j_{2n}}\rangle$ is $(\frac{1}{3})^n$ multiplied by the number of ways of pairing the indices.

Although the averaged spherical model leads to

the same expressions for the moments as does the spherical model, and therefore these are no easier to evaluate, in the form given by (31), we can easily evaluate the correlation function (24) by transforming (29) to a set of coordinates oriented along the value of $\vec{S}_0$.

By isotropy,

$$\langle S_q^\alpha(t) S_{-q}^\alpha(0)\rangle = \tfrac{1}{3}\langle \vec{S}_q(t)\cdot\vec{S}_{-q}(0)\rangle . \tag{32}$$

For each value of $\vec{S}_0$, we define a coordinate system with its z axis along $\vec{S}_0$. The time evolution is now very simple.

$$\begin{aligned} &\frac{\partial}{\partial t} S_q^0(t,\vec{S}_0) = 0 , \\ &\frac{\partial}{\partial t} S_q^{\pm1}(t,\vec{S}_0) = \pm i(J_0 - J_q) S_0 S_q^{\pm1}(t) , \end{aligned} \tag{33}$$

where $S_0 = |\vec{S}_0|$.

Thus

$$\begin{aligned} \vec{S}_q(t,\vec{S}_0)\cdot\vec{S}_{-q}(0,\vec{S}_0) = {} & S_q^0(0,\vec{S}_0) S_{-q}^0(0,\vec{S}_0) \\ & + \tfrac{1}{2}\cos[(J_0 - J_q)S_0]t[S_q^{-1}(0)S_{-q}^{+1}(0) \\ & + S_q^{+1}(0)S_q^{-1}(0)] \end{aligned} \tag{34}$$

Since the $\vec{S}_q$ are independent of $\vec{S}_0$,

$$\begin{aligned} &\tfrac{1}{2}\langle S_q^{-1}(0,\vec{S}_0) S_{-q}^{+1}(0,\vec{S}_0)\rangle \\ &\quad = \langle S_q^0(0,S_0) S_{-q}^0(0,S_0)\rangle = \rho_q \end{aligned} \tag{35}$$

and hence

$$R_q(t) = \tfrac{1}{3} + \tfrac{2}{3}\langle \cos[(J_0 - J_q)S_0 t]\rangle , \tag{36}$$

where the average in (36) is over the distribution

$$P(S_0) = 3(3/2\pi)^{1/2} S_0^2 e^{-3S_0^2/2} . \tag{37}$$

From (36) and (37) we have the relaxation function for the dynamical spherical model at $T=0$ (Fig. 10):

$$R_q(t) = \tfrac{1}{3} + \tfrac{2}{3} e^{-(\omega_q t)^2/6}[1 - \tfrac{1}{3}(\omega_q t)^2], \quad \omega_q = J_0 - J_q . \tag{38}$$

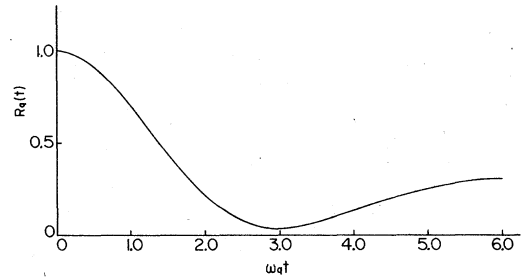

FIG. 10. Spin-spin correlation function in the dynamical spherical model at $T=0$.

The Laplace transform of $R_q(t)$ is

$$R_q(z) = \frac{i}{3z} + \frac{2}{3} i \int_{-\infty}^{\infty} \langle (z - \omega_q S_0)^{-1}\rangle \rho(S_0)\, dS_0 \tag{39}$$

and hence the spectral density is (Fig. 11)

$$\mathrm{Re}R_q(\omega + i\epsilon) = \frac{\pi}{3\omega_q}\delta\left(\frac{\omega}{\omega_q}\right) + (6\pi)^{1/2}\frac{\omega^2}{(\omega_q)^2} e^{-3/2(\omega/\omega_q)^2} . \tag{40}$$

It was not really necessary to introduce the averaged spherical model to obtain these results. They follow directly from Eq. (29) with $\vec{S}_0^\alpha$ defined as independent Gaussian random variables with a variance of $\frac{1}{3}$ and the assumption that the initial distribution of $\vec{S}_q$ is independent of $\vec{S}_0$. We have not, therefore, been particularly careful in showing (29) follows from the equations of motion. It is only necessary to observe that (29) may be solved in two ways, corresponding to the fixed-coordinate system and the system with $\vec{S}_0$ aligned along the z axis, and that the first choice leads to the moments obtained from the diagrammatic expansion of the spherical model, while the second choice permits the equations to be solved.

The treatment of the antiferromagnet is not significantly different. Referring again to Fig. 6 we will have the two choices $q_1 = q_c$, $q_2 = q - q_c$ and $q_1 = q - q_c$, $q_2 = q_c$. The value of the vertex is

$$i(J_{q_c} - J_{q-q_c})\epsilon^{\nu_1\nu_{q_c}\nu_{q-q_c}}\rho_{q-q_c}/\rho_q .$$

If $q = q_c$ we see that the vertex is zero since $\rho_0/\rho q_c$ vanishes as $T \to 0$. As before, the line that carries the wave vector q_c can only recombine with a right

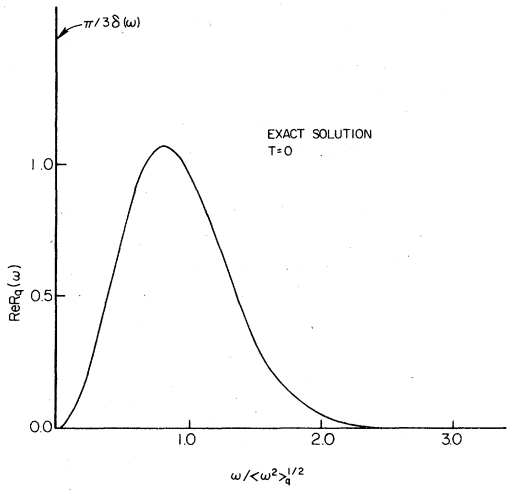

FIG. 11. Spectral density in the dynamical spherical model at $T=0$.

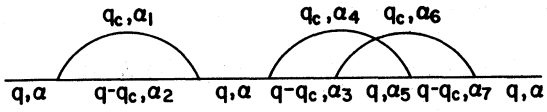

FIG. 12. Typical diagram for the antiferromagnet at $T=0$.

vertex. The next vertex which has the incoming wave vector $q-q_c$, has the value

$$i(J_{q_c}-J_q)\epsilon^{\nu_q\,-q_c^{\nu}\,q_c\,\nu_q}\rho_q/\rho_{q-q_c}.$$

We see that the factors of ρ_q from two consecutive vertices cancel. The structure of the diagrams is as shown in Fig. 12, with the vertices having alternately values proportional to $J_{q_c}-J_{q-q_c}$) and $J_{q_c}-J_q$. The rules for the calculating of the moments are identical, except that rule (ii) becomes (ii′): associate alternate factors of $i(j_{q_c}-j_{q-q_c}$ $-j_{q-q_c})\epsilon^{\nu i\nu q_c\nu f}$ and $i(J_{q_c}-J_q)\epsilon^{\nu i\,\nu\,q_c\nu f}$ with each vertex, beginning with the former. The solution is the same as (38) and (40), with the appropriate expression for ω_q.

We note that $\lim_{t\to\infty}\langle S_q(t)S_{-q}(0)\rangle=\frac{1}{3}$. This is true only at $T=0$. At any nonzero temperature, this limit would be zero.

III. DISCUSSION OF SOLUTION AND COMPARISON WITH THE HEISENBERG MODEL

The physical interpretation of the solution is evident from its derivation. We can regard the response of the system as the sum of a longitudinal and a transverse response (with respect to $\vec{S}_0$), of equal integrated intensities for each component. The longitudinal fluctuations are static at $T=0$, and are responsible for the finite value ($\frac{1}{3}$) of the correlation function (38) as $t\to\infty$. The transverse fluctuations are well-defined spin waves. However, since the magnitude of S_0 is not fixed, the spectrum that is seen is inhomogeneously broadened, and the line shape is given by the probability distribution of the magnitude of S_0. The solution satisfies the dynamical scaling hypothesis, and in fact a much stronger version, since the spectral function width scales with ω_q for all q, not just q(or q^*) $\ll\pi/a$. This latter feature is a peculiarity of the model, and does not hold for the dynamical spherical model in three dimensions or more.

It is interesting to compare the result with the nearest-neighbor Heisenberg model at $T=0$, where $\mathrm{Re}R_q(\omega)=\pi\delta(\omega^2-\omega_q^2)$. The entire weight is contained in the spin-wave lines, which are perfectly well defined, and there is no central resonance. The difference is readily understood. If we define S_0 in the same way, the constraint $\vec{S}_i\cdot\vec{S}_i=1$ requires that the distribution of S_0 at $T=0$ be $\delta(S_0-1)$. The spin waves are well defined since the magnitude of S_0 does not have any fluctuation. Also, the susceptibility along $\vec{S}_0$ is no longer equal to that transverse to $\vec{S}_0$. Spin-wave arguments would indicate that $\langle S_q^l S_{-q}^l\rangle\propto(KT)^2$, whereas $\langle S_q^{\perp}S_{-q}^{\perp}\rangle\propto KT$ for $q\gg k$. Hence $\langle S_q^l S_{-q}^l\rangle/\langle\vec{S}_q\cdot\vec{S}_{-q}\rangle=0$ at $T=0$, explaining the absence of a central resonance.[10] This latter argument also explains the difference between the susceptibilities for the Heisenberg and spherical model near $T=0$. We have, as $T\to 0$, for fixed q

$$\langle\vec{S}_q\cdot\vec{S}_{-q}\rangle_H=\frac{2KT}{J_0-J_q},\quad\langle\vec{S}_q\cdot\vec{S}_{-q}\rangle_{\mathrm{sph}}=\frac{3KT}{J_0-J_q}. \tag{41}$$

Let us assume that the spherical-model susceptibility gives correctly the transverse susceptibility in the Heisenberg model as well, if $q\gg k$, and that the longitudinal susceptibility is negligible. Then we would have

$$\langle\vec{S}_q\cdot\vec{S}_{-q}\rangle_H=\langle S_q^l S_{-q}^l\rangle_H+2\langle S_q^{\perp}S_{-q}^{\perp}\rangle_{\mathrm{sph}}=\tfrac{2}{3}\langle\vec{S}_q\cdot\vec{S}_{-q}\rangle_{\mathrm{sph}}, \tag{42}$$

which is the correct result.

The existence of well-defined spin waves in the Heisenberg model at $T=0$ has been shown only for the case that the interactions are nearest neighbor. The spherical model is known to give the same static critical behavior as the Heisenberg model in the limit that the interaction becomes long ranged, and does not have perfectly well-defined spin waves at $T=0$. It is interesting to ask what happens to the spin waves in the Heisenberg model if the interaction is long ranged. For instance, does a small amount of next-nearest-neighbor interactions lead to a small linewidth at $T=0$? The answer to this question is no. For any finite range of interaction, the Heisenberg model yields well-defined spin waves at $T=0$. To see this, we observe that the equations of motion can be written

$$\frac{\partial^2 S_q}{\partial t}=-\sum\Gamma(q_1q_2q_3)\delta(q_1+q_2+q_3-q)S_{q_1}^{\alpha}\vec{S}_{q_2}\cdot\vec{S}_{q_3}, \tag{43}$$

where

$$\Gamma(q_1q_2q_3)=\tfrac{1}{2}N^{-1}[(J_{q_1+q_3}-J_{q_2}(J_{q_1}-J_{q_3})+(J_{q_1+q_2}-J_q)(J_{q_1}-J_{q_2})]. \tag{44}$$

It is readily verified that the correct spin-wave frequency in the nearest-neighbor chain is obtained by replacing the operator $\vec{S}_{q_2}\cdot\vec{S}_{q_3}$ by its average evaluated at $T=0$, i.e.,

$$\vec{S}_{q_2}\cdot\vec{S}_{q_3}\to\langle\vec{S}_{q_2}\cdot\vec{S}_{q_3}\rangle=N\delta(q_2-q_c)\delta(q_3+q_c)S^2, \tag{45}$$

leading to

$$\frac{\partial^2 S_q}{\partial t^2}=-\omega_q^2 S_q, \tag{46}$$

where

$$\omega_q^2 = (J_{q+q_c} - J_{q_c})(J_{q_c} - J_{q_c})S^2 . \quad (47)$$

This replacement is asymptotically exact because the fluctuation

$$\delta\vec{S}_{q_2} \cdot \vec{S}_{q_3} = \vec{S}_{q_1} \cdot \vec{S}_{q_2} - \langle \vec{S}_{q_1} \cdot \vec{S}_{q_2} \rangle \quad (48)$$

vanishes, that is, takes nonzero values with vanishing probability as $T \to 0$. In fact, for nearest-neighbor Heisenberg chains, one can show that

$$\langle (\delta\vec{S}_i \cdot \vec{S}_j)^2 \rangle = (\kappa |r_i - r_j|)^2 S^4, \quad K|r_i - r_j| \ll 1 \quad (49)$$

where K, the inverse coherence length, is KT/JS^2a. The condition $\kappa|r_i - r_j| \ll 1$ will always be satisfied for the sites appearing in the equation of motion (43), if κ is sufficiently small. The distance between sites is limited by the range of the interaction to at most two, for nearest-neighbor interactions, and more generally, to twice the range of the interaction.

We will assume that the interaction is actually zero beyond some distance, to avoid problems with limits that we wish to exclude from the present discussion. Then a sufficient condition for the existence of perfectly-well-defined spin waves is that $\delta\vec{S}_i \cdot \vec{S}_j \to 0$ for i and j any fixed distance apart, as $T \to 0$.

Let

$$\vec{\Delta}_j = \vec{S}_j - \langle \vec{S}_i \cdot \vec{S}_j \rangle S^{-2} \vec{S}_i , \quad (50)$$

then

$$\delta\vec{S}_i \cdot \vec{S}_j = \Delta_j \cdot \vec{S}_i . \quad (51)$$

From the Schwartz inequality

$$\langle (\vec{S}_i \cdot \vec{\Delta}_j)^2 \rangle \leq \vec{S}_i \cdot \vec{S}_i \vec{\Delta}_j \vec{\Delta}_j = S^4 (1 - \langle \vec{S}_i \cdot \vec{S}_j \rangle^2 S^{-4}) . \quad (52)$$

Hence as long as the interaction is such as to lead to ferromagnetic or antiferromagnetic order, so that $\langle \vec{S}_i \cdot \vec{S}_j \rangle^2 \to S^2$ when $T \to 0$, the fluctuation $\delta\vec{S}_i \cdot \vec{S}_j$ will vanish, and the excitations at $T = 0$ will be perfectly-well-defined spin waves. Interactions that lead to helical ordering, for which $J(q)$ has a maximum at a wave vector q_c other than $q_c = 0$ or $q_c = \pi/a$ require further analysis. Adding a small amount of next-nearest-neighbor interaction to a nearest-neighbor system does not, however, lead to a finite linewidth.

In the spherical model, one can show that

$$\langle (\delta\vec{S}_i \cdot \vec{S}_j)^2 \rangle = \tfrac{1}{3}(1 + \langle S_i S_j \rangle^2) \quad (53)$$

and so the criterion for the existence of spin waves fails. In fact, when $i = j$, the criterion $\delta\vec{S}_i \cdot \vec{S}_i = 0$ is simply the statement that the spins are of fixed length, which is violated in the spherical model, and as we have seen, it is precisely the fluctuation in the length that is responsible for the linewidth at $T = 0$. From a formal point of view, the constraint $\vec{S}_i \cdot \vec{S}_i = 1$ leads to nonvanishing four- (and higher-) spin cumulants, that are not present in the spherical model. These in term, lead to additional decay processes, discussed in Sec. I, that are responsible for the well-defined spin waves at $T = 0$, in one dimension. We would expect, in higher dimensions, that these correlations will also significantly affect the sharpness of the spin waves. Approximate methods, using only the vertices of the spherical model, and hence neglecting these correlations, do not show the three-peaked structure observed in the three-dimensional Heisenberg antiferromagnet $RbMnF_3$,[14] yielding only a broad central resonance, even when these calculations are taken beyond and mode-coupling approximation to include the lowest-order scattering process of Fig. 2(d).[15] We examine these methods and the extended-mode-coupling theory as they apply to the one-dimensional case in Sec. IV.

IV. VALIDITY OF APPROXIMATE SOLUTIONS

The existence of a known exact solution provides the possibility of exploring the validity of the extended-mode-coupling theory treated as a scheme of successive approximations. The first approximation, the mode-coupling theory, or independent-mode approximation has been used extensively in magnetic systems and fluids at the critical point,[5] in ordinary fluid turbulence,[16] and in plasma turbulence.[17]

Despite its successes in practical calculations, it is widely recognized that these theories are less than satisfactory, there being no *a priori* reason for suspecting that the higher-order terms are small, as there is no expansion parameter.[18] There is only the intuitive sense that very complex processes for the buildup of correlations are unlikely to have a profound effect on the dynamics of a single mode. One might expect that spectral functions obtained by taking more and more terms in the expansion of the self-energy in renormalized skeleton diagrams (extended-mode-coupling expansion) would converge to the correct spectral function. The difficulty of doing the calculations, and to our knowledge, none have been done past the second term in the expansion, has precluded any systematic investigation of the convergence properties by direct calculation. It is a relatively simple matter, for the spherical model chain to investigate these approximations. One cannot automatically infer that the results obtained in one dimension at $T = 0$ are applicable as well to the other situations we have mentioned, although we suspect that is so.

The contribution of any skeleton diagrams con-

taining $2n=2$ vertices may be seen to be, for $n>0$,

$$\phi_q^{2n+2}(t)=\pm i(\omega_q)^{2n+2}\int_0^t\cdots\int_0^{t_3}\int_0^{t_2}dt_1\,dt_2\cdots dt_{2n}\,G_q(t_1)G_q(t_2-t_1)\cdots G_q(t-t_{2n})\,. \tag{54}$$

The equation of motion can be written

$$-izG_q(z)=1-i\phi_q(z)G_q(z)\,, \tag{55}$$

which upon expanding $\phi_q(z)$ in renormalized skeleton diagrams leads to

$$-izG_q(z)=1-\sum_{n=1}^{\infty}A^{2n}(\omega_q)^{2n}[G_q(z)]^{2n}\,, \tag{56}$$

where A^{2n} is the sum of all skeleton diagrams with $2n$ vertices. Defining

$$G^*(z^*)=(1/\tfrac{2}{3}\omega_q)G(z^*/\tfrac{2}{3}\omega_q)\,,$$

we find that $G^*(z)$ satisfies

$$-izG^*(z)=1-\sum_{n=1}^{\infty}(\tfrac{3}{2})^n A^{2n}[G^*(z)]^{2n}\,. \tag{57}$$

We have chosen the normalization so that the second moment of $G^*(z)$ is 1. All reference to the wave vector has dropped out. That this is possible is the statement of dynamical scaling, although here it is much stronger, since the result holds as well for large values of q.

For the antiferromagnet we require two equations for $G_q(z)$ and $G_{k_0-q}(z)$, but since $\omega_q=\omega_{k_0-q}$, these two functions are identical, and we obtain Eq. (57) for the scaled function.

It can be seen from the discussion in the Introduction, or directly from (56) by expanding both sides in powers of $1/z$, that the solutions of the equation one obtains by truncating the series after A^{2n}, will have the first $2n$ moments of the spectral function correct.[1] For instance, the mode-coupling approximation corresponds to solving

$$-izG^*(z)=1-[G^*(z)]^2 \tag{58}$$

or

$$G^*(z)=\tfrac{1}{2}[iz\pm(4-z^2)^{1/2}]\,. \tag{59}$$

The appearance of multiple roots indicates that the solutions of (57) are not unique. The solutions of the analog of (57) in the time domain are unique, if we require $G(t)$ to be a continuous function, since one can obtain a convergent Taylor-series expansion by solving the equations iteratively. The appearance of additional solutions of the Laplace-transformed equations corresponds to admitting singular solutions in the time domain. For instance, one choice of sign in (59) leads to a $G^*(z)$ such that

$$\lim_{z\to\infty}G^*(z)=iz\,. \tag{60}$$

The limiting form corresponds to the solution in the time domain $G^*(t)=-\partial\delta(t)/\partial t$, which one readily checks, is a solution, with $G^*(0)=0$, and

$$\frac{\partial G^*(t)}{\partial t}=-\int_0^t G^*(t-t')G^*(t')\,dt'\,, \tag{61}$$

the equation of motion in the time domain corresponding to (58). Higher-order polynomials used to approximate $\phi_q(z)$ yield additional spurious solutions. There will always be one solution that approaches i/z, as $z\to\infty$, and it is the zero of the polynomial equation that goes continuously into this one as $z\to\infty$ that we identify with the physical solution. We must therefore choose the negative imaginary square root in (59). We see then that the high-frequency expansion of $G^*(z)$ is

$$G^*(z)=(i/z)(1+1/z^2+1/z^4+\cdots)\,, \tag{62}$$

which does indeed have the correct second moment. It follows from a Taylor-series expansion of (44) that the exact $G^*(z)$ can be expanded

$$G^*(z)=(i/z)(1+z^{-2}+\tfrac{5}{2}z^{-4}+\tfrac{70}{8}z^{-6}+\tfrac{315}{8}z^{-8}+\tfrac{3465}{16}z^{-10}+\cdots)\,, \tag{63}$$

so the fourth (and higher) moments of (59) are not correct, which can be seen by comparing (63) and (62).

Using the exact solution to generate the coefficients A^{2n} by the requirement that they give the correct moments (for A^4 and A^6 these have also been obtained by adding graphs) we obtain the extended-mode-coupling equation of motion, through terms containing 10 vertices:

$$-izG^*(z)=1-[G^*(z)]^2+\tfrac{1}{2}[G^*(z)]^4-\tfrac{3}{4}[G^*(z)]^6+\tfrac{35}{8}[G^*(z)]^8-\tfrac{467}{8}[G^*(z)]^{10}+\cdots\,. \tag{64}$$

For real z, this polynomial equation may be readily solved for its roots by squaring it and utilizing standard routines for finding the roots of a polynomial with real coefficients. For imaginary z, the roots may be found directly. If we keep only the terms up to $[G^*(z)]^n$, we obtain the results shown in Fig. 13. The solutions are not reproducing the central peak and sidebands observed in the exact solution. The results of including the terms with $n\geq 6$ are particularly interesting. It may be

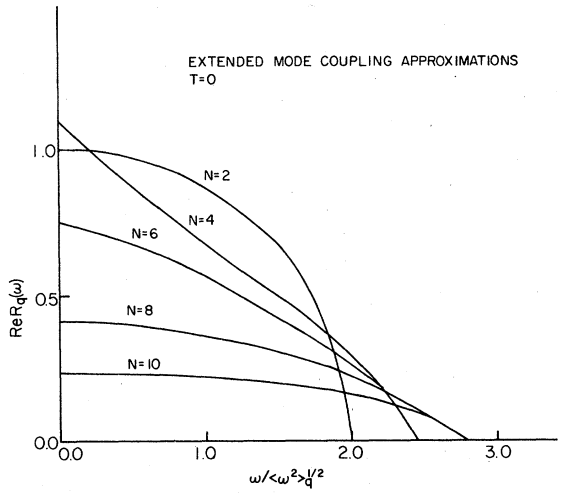

FIG. 13. Spectral density obtained from the extended-mode-coupling approximations with n vertices in the self-energy.

noted that the area under the curve, which should be $\frac{1}{2}\pi$ in all cases, is too small for $n \geq 6$. The reason for this is that these solution do not satisfy the Kramers-Kronig relation, as they are not analytic in the upper half plane. This may be seen by comparing the values of $G^*(z)$ one obtains by moving to $z=0$ from large values of z along the real and imaginary axis (see Table I). Although in both cases, the solution approaches iz^{-1} for large z, the value approached at $z=0$ is not the same for the two paths. There is no way of analytically continuing the root of the polynomial equation for large z that behaves as i/z, so that it is in an analytic function in the entire half plane. There must be a branch point in the first quadrant for the function which is a root for all z. A singularity in the upper half plane can only occur if the function $G^*(t)$ is not bounded as $t \to \infty$. There is therefore, no physically reasonable solution of the equation with terms up to the sixth included.

TABLE I. Values of $G(z)$ for z along imaginary $[\mathrm{Re}G(i\tau)]$ and real $[G(\omega)]$ axes. Observe that $\lim_{\tau\to 0} G(i\tau) \neq \lim_{\omega\to 0} G(\omega)$.

	$N=8$		
τ,ω	$\mathrm{Re}G(i\tau)$	$\mathrm{Re}G(\omega)$	$\mathrm{Im}G(\omega)$
0	0.756	0.406	0.765
0.4	0.731	0.390	0.738
0.8	0.707	0.369	0.707
1.2	0.619	0.337	0.669
1.6	0.494	0.287	0.630
2.0	0.420	0.214	0.600
2.4	0.365	0.107	0.507
2.8	0.322	0	0.435
3.2	0.287	0	0.355
3.6	0.260	0	0.305
4.0	0.236	0	0.269

This rather startling result is unexpected but not one that we have any *a priori* claim to rule out. By truncating the series for the self-energy, we sum a subset of diagrams, and generate a sequence of approximate moments, that need not correspond to a physically realistic relaxation function.

It is possible that it is the peculiar nature of the critical point in one dimension that is responsible for this lack of regularity in the extended-mode-coupling approximation. In particular, the limiting spectral function is a distribution, not a function. We suspect that this is not the case, and that the irregular behavior exhibited here extends to higher dimensions and more-general systems. Consider for instance the effect of a small temperature on the spectral function, for $q \gg \kappa$ $(q^* \gg \kappa)$. The exact result will be much like Fig. 10, the primary difference being that there will be a width to the central peak. The moments are all continuous functions of κ, so that the $t=0$ value of the diagrams will change continuously. It will no longer be possible to represent the frequency dependence of the diagrams by a simple product, and we must take convolutions, but these will have widths on the order of $\kappa^2(\kappa)$ for the ferromagnet (antiferromagnet) and for time on the order of q^2, (q) we would expect only small changes in the resultant solution. Therefore, except possibly for the central-peak region, the solution for any n, must be continuous with that at $T=0$, and hence converge as poorly to the correct result.

The inadequacy of methods based upon the self-consistent solution of renormalized diagrams has been observed by Kraichnan[19] in a class of stochastic models he has constructed that allowed him to investigate this question, reinforcing our sense that the failure of these methods is not restricted to the particular systems considered. If indeed it is correct that including higher-order diagrams does not yield a convergent series of solutions at higher temperatures or more generally, with different expressions for the q dependence of the vertices, then it is a defect of the resummation procedure that is inherent in the structure of the diagrams. The significance of the lower-order solutions is then open to question, at least in the sense in which they are to be interpreted as approximations. It is one thing for the mode-coupling approximation to be the first in a series of approximations that converges to a solution, and quite another to be the first in a series of approximations that does not converge to anything. It should

be noted, however, that the scaling exponent z is given correctly even if the series is not convergent, and it is only the shape of the scaling function which is in question.

We wish now to consider other approximate means of calculating spectral functions. There is no compelling reason why the renormalization and use of skeleton diagrams need be carried out at the level of the self-energy $\phi_q(z)$. One can just as readily use a terminated continued fraction, and develop the self-energy that appears in a series of renormalized skeleton diagrams. For instance, one can write as an exact result,

$$G_q(z) = i\{z - \omega_q^2/[z - V_q(z)]\}^{-1}, \tag{65}$$

where $V_q(z)$ is shown diagrammatically in Fig. 14. The crosshatched box indicates that all diagrams containing three or more lines in the intermediate state are summed. The vertices shown explicitly do not have associated a factor of z^{-1}, all vertices within the cross hatched region do, and there is one overall factor of z^{-1}. $V_q(z)$ is the self-energy governing the decay of the spin current.

This result may be derived using projection operators or diagrammatically. Here again, one may develop the diagrams in terms of renormalized lines and skeleton diagrams. The lowest-order approximation would be to make the replacement shown in Fig. 14(b). At $T=0$, this reduces the diagrams needed to those of Fig. 14(c), and we have explicitly

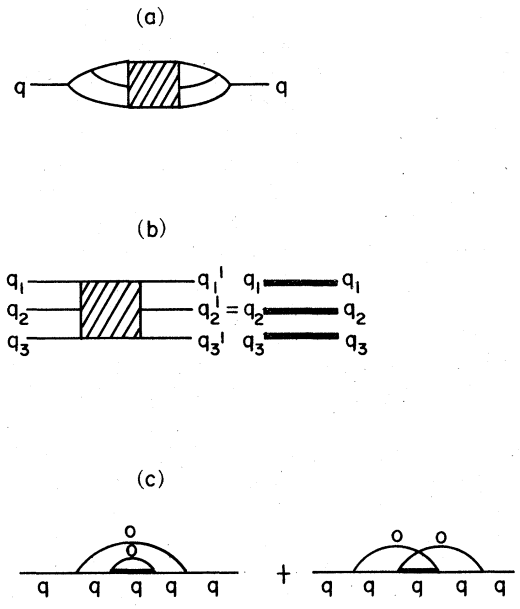

FIG. 14. (a) Self-energy $V_q(z)$. (b) The independent-mode approximation for the correlation function appearing in $V_q(z)$. (c) The approximate expression for $V_q(z)$ obtained using the independent-mode approximation.

$$V_q(z) = -i(\langle\omega_q^4\rangle - \langle\omega_q^2\rangle^2)G_q(z). \tag{66}$$

We note that dynamical scaling for $G_q(z)$ follows as well from this expansion as it does from the mode-coupling expansion. The scaled function satisfies

$$G^*(z) = i\{z - [z + i\tfrac{3}{2}G^*(z)]^{-1}\}^{-1} \tag{67}$$

or

$$G^*(t) = \frac{i}{3z}(z^2 + \tfrac{1}{2}) \pm \frac{i}{3z}[(z^2 + \tfrac{1}{2})^2 - 6z^2]^{1/2}. \tag{68}$$

In order to have $\lim_{z\to\infty} G^*(z) = iz^{-1}$, we must choose the negative sign for large values of z. If this choice is retained for $z \to 0$, we will obtain $G^*(0) = 0$. However, when the argument of the square root is zero, the two branches of the solution join, and we can construct a solution that passes from one branch to the other. The choice of the positive sign for $z \leq \frac{1}{2}[5 - (24)^{1/2}]$, leads to $\lim_{z\to\infty} G^*(z) = i/3z$. The singularity at $\omega = 0$ of the exact solution is thus reproduced, with the correct strength. The solution is plotted in Fig. 15, ($n=4$), and we see that it is qualitatively correct, the sloppy-spin-wave sidebands being reproduced, as well as the central peak. The improvement over the extended-mode-coupling result is dramatic, and this approximation may in fact prove to be of value for calculating the scaling functions in three dimensions.

One may continue the approximations in two directions. Additional skeleton diagrams may be included in the expansion of $V_q(z)$. We find by comparing moments with the exact solution that the next approximation for $G^*(z)$ would be

$$G^*(z) = i[z - 1/(z + i\{\tfrac{3}{2}G^*(z) - [G^*(z)]^3\})]^{-1}. \tag{69}$$

This may be solved by the same methods as used previously for the extended-mode-coupling approximation, and the result is also shown in Fig. 15 ($n=6$).

The solution is in no sense a better approximation than that attained from (65). In particular, note that the solution that is singular at the origin does not have the correct strength, as one may infer from (69) by observing that $\lim_{z\to 0} G^*(z) = iz^{-1}$ is consistent. Keeping higher-order terms in the expansion will not alter the strength of this singularity. We have shown in Fig. 15 the result of solving (67) ($n=6$) and of the equation one gets by including the next-order terms ($n=8$). It is clear that the solution gets worse as one includes more terms, rather than better.

The other direction that one might seek as improvement of the approximation given by (66) is to extend the continued-fraction expansion before evaluating the final self-energy.

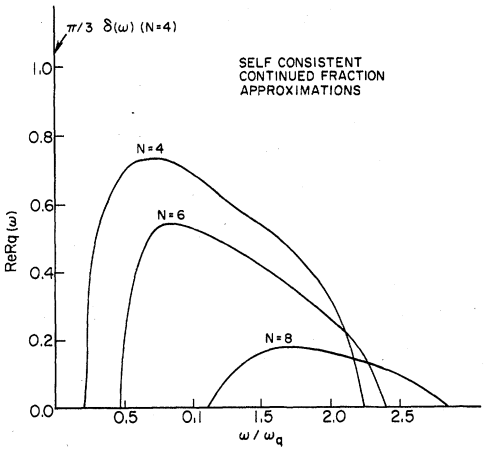

FIG. 15. Spectral density obtained using approximations for $V_q(z)$. n denotes the number of vertices in the skeleton diagrams. The diagrams for $n=4$ are shown in Fig. 13(c), $n=6$ corresponds to Eq. (69).

In this way, if we keep only the first term in the expansion of the final self-energy in skeleton diagrams, we obtain an approximation of the form

$$G^*(z) = \cfrac{i}{z - \cfrac{1}{z - \cfrac{3/2}{z - \cfrac{a_3}{z - \ddots \; z - \cfrac{a_{n-1}}{z + i a_n G^*(z)}}}}} \,. \tag{70}$$

If n is odd, we obtain for $G^*(0)$ the result

$$G^*(0)^2 = \prod_{k=0}^{(n-1)/2} a_{2k} \Big/ \prod_{k=0}^{(n-1)/2} a_{2k+1} \tag{71}$$

with $a_0 = 1$, while if n is even, we obtain

$$G^*(0) = -G^*(0) \prod_{k=0}^{n/2} a_{2k+1} \Big/ \prod_{k=0}^{n/2} a_{2k} \,. \tag{72}$$

Since the a's are all positive, this will have as a solution $G^*(0)=0$, and (70) may also yield a singular solution, as we have seen.

It is clear that unless the quotient in (71) converges to zero, which it does not appear to do in this case, the series of approximations obtained from (70) cannot converge to anything. The next approximation to (65) with $n=3$, $a_3=2/3$, is not qualitatively correct, being regular at $z=0$, and showing no sidebands, with the entire spectrum localized around $z=0$. Thus, whichever way the approximation method is continued beyond the result contained in (65), the solution deteriorates, rather than improves.

We note that the kinetic theory developed by the

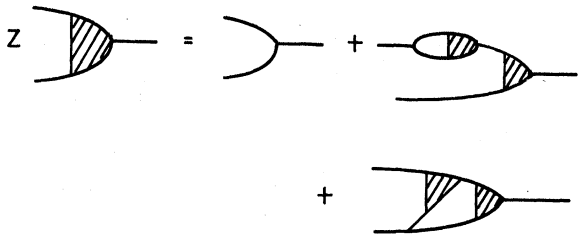

FIG. 16. Self-consistent equation for the vertex function used in the kinetic theory of the Heisenberg paramagnet.

author[3] can also be solved exactly at $T=0$. This theory is a self-consistent equation for the vertex function, shown in Fig. 16, rather than $G^*(z)$. It has the virtue of being consistent with energy conservation, and gives a solution for $G^*(z)$ which has correct moments up to the fourth. It has given a good quantitative description of the spectral functions in three-dimensional antiferromagnets away from T_c.[14] We find, however, that the solution in this case at $T=0$ is close to that given by the extended-mode-coupling result for $n=4$ (see Fig. 13), and therefore is qualitatively incorrect.

We have not considered summing infinite sets of diagrams, such as done by Fedders[20] for the limit of infinite dimension and infinite temperature, and it is possible that a procedure can be found that will eliminate the convergence difficulties in the extended-mode-coupling expansion in a similar fashion, at finite temperatures.

V. CONCLUSION

An exact solution, obtainable by summing all the diagrams in the moment expansion of the spectral function, exists for the dynamical spherical model at $T=0$. The solution is readily understood in terms of a model in which spin waves propagate transverse to a uniform magnetization, whose orientation is arbitrary and whose magnitude is simply related to a Gaussian random variable. As a consequence of the fluctuation in the magnitude of this effective magnetization, the spin-wave spectrum is inhomogeneously broadened, and the spin waves have a finite lifetime at $T=0$. The fluctuations parallel to this magnetization do not decay (at $T=0$) and are responsible for the finite value at $t=\infty$ of the spin-spin correlation function, and the corresponding pole at $\omega=0$ in the spectral density.

In the Heisenberg model, the constraint that the spins be of fixed length eliminates the inhomogeneous broadening and causes the longitudinal susceptibilities to vanish relative to the transverse, leading to perfectly-well-defined spin waves and the absence of a central peak. The constraint is

incorporated in the microscopic treatment of the dynamics by the presence of additional decay vertices, reflecting the existence of non-Gaussian correlations in equilibrium. These vertices are comparable to, and exactly cancel, at $T=0$, the contribution from the vertices arising from the Gaussian part of the fluctuations, explaining the failure of the mode-coupling theory to predict an infinite lifetime for spin waves in the Heisenberg chain at $T=0$.

The solution for the spherical model satisfies the dynamical scaling hypothesis, with a dynamical exponent of $z=2$ for the ferromagnet and $z=1$ for the antiferromagnet. A perturbation expansion of the self-energy, ordered in terms of the number of vertices in dressed skeleton diagrams, the extended-mode-coupling theory, is consistent, term by term, with the dynamical scaling hypothesis, with the correct exponents, but yields scaling functions that are qualitatively incorrect in lower orders, and physically unrealistic in higher orders.

The best approximation we have found uses the lowest-order mode-coupling approximation (independent-mode approximation) for the self-energy of the spin current. It gives a qualitatively correct solution, and will perhaps be of value in three dimensions. The solution deteriorates if one attempts to go to higher orders in the number of interactions in the self-energy. There does not appear to be any scheme for utilizing the lower-order perturbation results to obtain a convergent series of approximations to the exact solutions, at least, using a finite number of diagrams.

Note added in proof. The results obtained here are valid in two dimensions. In particular, the correlation function is given by (38) and (40) with the appropriate expressions for ω_q. This is readily seen by observing that the essential feature of the derivation was that

$$\langle \vec{S}_q \circ \vec{S}_{-q} \rangle \xrightarrow[T\to 0]{} \delta(q-q_c)\,,$$

which is true in two dimensions as well as in one.

ACKNOWLEDGMENTS

I would like to thank Alf Sjolander for valuable conservations, encouragement, and the suggestion of the average spherical model, Edgar Rieflin for valuable conversations in the later stages of this work, Att Lagendijk for an insightful comment on the manuscript, and F. C. Barreto and the members of the Physics Department of Universidade Federal de Minas Gerais for their kindness and hospitality.

APPENDIX A: PROOF OF STATIONARITY OF THE SPHERICAL-MODEL DISTRIBUTION

We wish to show that the spherical-model distribution given by (5) is stationary when the spin components evolve according to the equations of motion (2). It will be more convenient to use Fourier-transformed variables

$$S_q^\alpha \equiv N^{-1/2} \sum e^{iqr_i} S_i^\alpha . \tag{A1}$$

We want to show then that

$$\frac{\partial}{\partial t} \langle S_{q_1}^{\alpha_1} \cdots S_{q_n}^{\alpha_n} \rangle \Big|_{z=0} = 0 . \tag{A2}$$

When n is even, (A2) is trivially true, since the time derivative involves the average of an odd number of operators, and this will vanish. We need only consider the case that n is odd. For $n=1$, translation invariance assures the result. The first nontrivial case is $n=3$. The spherical indices $\pm 1, 0$ are more convenient. The equations of motion are

$$\begin{aligned} \frac{\partial S_q^{\pm 1}}{\partial t} &= \pm N^{-1/2} i \sum_{q'} (J_{q-q'} - J_{q'}) S_{q'}^z S_{q-q'}^{\pm 1} , \\ \frac{\partial S^0}{\partial t} &= \frac{N^{-1/2}}{2} \sum_{q'} (J_{q-q'} - J_{q'}) S_{q'}^- S_{q-q'}^+ . \end{aligned} \tag{A3}$$

It is a consequence of (5) that

$$\langle S_{q_1}^{\alpha_1} \cdots S_{q_{2n}}^{\alpha_{2n}} \rangle = \sum \langle S_{q_{i_1}}^{\alpha_{i_1}} S_{q_{i_2}}^{\alpha_{i_2}} \rangle \cdots \langle S_{q_{i_{2n-1}}}^{\alpha_{i_{2n-1}}} S_{q_{i_{2n}}}^{\alpha_{i_{2n}}} \rangle , \tag{A4}$$

where $\{P\}$ is the sum over all pairings of the $2n$ indices. The correlation functions vanish, by rotation and translation invariance unless $\sum \alpha_i = 0$ and $\sum q_i = 0$.

Taking the time derivative of each operator separately, using (A4) in the result, together, with the criterion that $\sum \alpha_i = 0$, $\sum q_i = 0$ for all the correlation functions, we obtain

$$\frac{\partial}{\partial t} \langle S_{q_1}^0 S_{q_2}^0 S_{q_3}^0 \rangle = 0 , \tag{A5}$$

$$\begin{aligned} \frac{\partial}{\partial t} \langle S_{q_1}^{-1} S_{q_2}^0 S_{q_3}^{+1} \rangle = {} & (J_{q_1} - J_{q_2}) \rho_{q_1} \rho_{q_3} + (J_{q_2} - J_{q_3}) \rho_{q_2} \rho_{q_3} \\ & + (J_{q_3} - J_{q_1}) \rho_{q_3} \rho_{q_1} , \end{aligned} \tag{A6}$$

where

$$\rho_q = \langle S_q^0 S_{-q}^0 \rangle = \tfrac{1}{2} \langle S_q^{-1} S_{-q}^{+1} \rangle .$$

In order that (5) be stationary, (A6) must be zero. This is a strong restriction on the form of the correlation function, which is satisfied by

$$\rho_q = (\alpha_1 + \alpha_2 J_q)^{-1} \tag{A7}$$

with α_1 and α_2 arbitrary. It can be shown that this is the only solution of (A6).

The restriction that $\sum \langle \vec{S}_i \cdot \vec{S}_i \rangle = 1$, or $3N^{-1} \sum_q \rho_q = 1$, restricts the possible form of $\rho(q)$ to a one-param-

eter family of functions. If we identify this parameter as β, the solution may be written, identifying also α_1/α_2 as $-\mu$ of (5):

$$\rho_q = \beta^{-1}(\mu - J_q)^{-1} = \beta^{-1}(\chi_{k_0}^{-1} + J_{k_0} - J_q)^{-1}, \qquad \text{(A8)}$$

where k_0 is arbitrary. χ_{k_0} is the static susceptibility at this wave vector, and is a function of β. This is the pair correlation function of the spherical model. This remarkable fact, that one can determine a static distribution from the requirement of stationarity, is not completely understood.

To complete the demonstration that (5) is indeed stationary it is required to show that (A2) holds for all $n > 3$. Consider $n = 5$. Then if there are not three spin variables in the average such that $\sum \alpha_i = 0$, $\sum q_i = 0$, the time derivative will vanish trivially, since the time derivative of one spin variable of wave vector q_{i_1} introduces two variables into the average that must be paired with two of the remaining four. There may be more than one triplet for which this condition holds. Consider first that there is only one. Say

$$\frac{\partial}{\partial t} \langle S^0_{q_1} S^{-1}_{q_2} S^{+1}_{q_3} S^0_{q_4} S^0_{-q_4} \rangle$$

with $q_1 + q_2 + q_3 = 0$. Then pairs of variables in the time derivative of $S^{\alpha}_{q_2}$, $i = 1, 2, 3$ can be paired only with the other two elements of the triplet and the time derivatives of the remaining two fluctuations cannot paired at all. The time derivative reduces to

$$\frac{\partial}{\partial t} \left(\langle S^0_{q_1} S^{-1}_{q_2} S^{+1}_{q_3} \rangle\right) \langle S^0_{q_4} S^0_{-q_4} \rangle$$

which has been shown to be zero. Suppose now that there is more than one way of finding such a triplet, and consider the spins that participate in more than one triplet. For instance

$$\frac{\partial}{\partial t} \langle S^0_{q_1} S^{-1}_{q_2} S^{+1}_{q_3} S^0_{q_1} S^0_{-q_1} \rangle .$$

The pairings necessary to associate the time derivative of $S^{-1}_{q_2}$ with one or the other factor $S^0_{q_1}$, are distinct, and the average of the six spins involved is the sum of all possible pairings. Therefore the time derivative of $S^{-1}_{q_2}$ is the sum of two terms, each being of the form

$$\frac{\partial}{\partial t} \langle S^0_{q_1} S^{-1}_{q_2} S^{+1}_{q_3} \rangle \langle S^0_{q_1} S^0_{-q} \rangle .$$

One obtains, therefore, that this time derivative is

$$2 \frac{\partial}{\partial t} \left(\langle S^0_{q_1} S^{-1}_{q_2} S^{+1}_{q_3} \rangle\right) \langle S^0_{q_1} S^0_{-q_1} \rangle$$

which vanishes.

In general, for arbitrary n, we will obtain

$$\frac{\partial}{\partial t} \langle S^{\alpha_1}_{q_1} \cdots S^{\alpha_{2n+1}}_{q_{2n+1}} \rangle = \sum_p \frac{\partial}{\partial t} \langle S^{\alpha_{i_1}}_{q_{i_1}} S^{\alpha_{i_2}}_{q_{i_2}} S^{\alpha_{i_3}}_{q_{i_3}} \rangle \times \langle S^{\alpha_{i_4}}_{q_{i_4}} S^{\alpha_{i_5}}_{q_{i_5}} \rangle \cdots \langle S^{\alpha_{i_{2n+1}}}_{q_{i_{2n+1}}} S^{\alpha_{i_{2n+2}}}_{q_{i_{2n+2}}} \rangle \qquad \text{(A9)}$$

where $\sum_p$ is the sum of all possible ways of choosing a triplet and $n-1$ pairs such that $\sum \alpha_i = 0$, $\sum q_i = 0$, and the remaining indices are paired.

APPENDIX B: COMPARISON OF MICROSCOPIC RESULTS WITH MODE-COUPLING THEORY

The basic equation of the mode-coupling approach for treating the long-wavelength fluctuations in the isotropic Heisenberg ferromagnet is[5]

$$\left(\frac{\partial}{\partial t} + \frac{q^2 L^0_q}{\chi_q}\right) \vec{S}_q = \frac{KT}{2N} (\chi_k^{-1} - \chi_{q-k}^{-1}) \vec{S}_k \times \vec{S}_{q-k} . \qquad \text{(B1)}$$

The sum is only over the "long" wavelengths $0 \leq |\vec{K}| \leq |\vec{K}_M|$, where $|K_M|$ is somewhat arbitrary but $\ll \pi/a$. L^0_q, the bare transport coefficient, is regarded as arising from the contributions of the "short"-wavelength fluctuations to the memory kernel $\phi_q(z)$ of the text. It is thought of as frequency independent, since (B1) will be used only to treat the low-frequency response, where $\vec{S}_q(t)$ varies on a time scale much longer than that of the modes that contribute as intermediate states in $\phi_q(z)$, to L^0_q.

Since

$$KT(\chi_k^{-1} - \chi_{q-k}^{-1}) = J_k - J_{q-k} \qquad \text{(B2)}$$

when the spherical-model expressions (A8) are used for the susceptibilities, (B1) reduced to the equation one obtains directly from the equations of motion, by transforming (2),

$$\frac{\partial \vec{S}_q}{\partial t} = \sum_k J_k \vec{S}_k \times \vec{S}_{q-k} \qquad \text{(B3)}$$

insofar as the mode-coupling terms are concerned. In order to calculate correlation functions from (B1), it is assumed that the S^{α}_q are Gaussian variables at $t = 0$. This is, of course, an approximation for the Heisenberg model. One then obtains a perturbation series for the self-energy in terms of bare propagators, the graphical series for the self-energy in terms of bare propagators, the graphical expansion for which would be identical to the one we have given, except that the bare lines would have a different significance, as the bare propagator is $i(z + q^2 L^0_q/\chi_q)^{-1}$, rather than iz^{-1}, and the summations are only over long-wavelength modes. When self-energy insertions are resummed, the formal expressions for the

self-energy in terms of the renormalized propagators will be identical with the ones we have given. The inverse propagator will be

$$(G_q^0)^{-1} = i^{-1}[z + iL^0 q^2/\chi_q - \phi_q(z)] \quad \text{(B4)}$$

but since for small q, the bare term is negligible, compared to $\phi_q(z)$ the mode-coupling solution would be identical to the result of the microscopic calculation.

There is evidently no reason to make the decomposition into long and short wavelengths for treating the spherical model, where the Gaussian assumption is exact, and can be used with (B3) to generate the self-consistent equations for the propagator. We note that Kawasaki's equations for the antiferromagnet[5] 5.105–5.107 appear more complicated than (B1) only because of the necessity of restricting the summations to the appropriate regions around $q=0$, $q=\pi/a$, and reduce to (B1) if these restrictions are lifted. Our preceding comments apply as well, then, to the antiferromagnet.

We have seen that the Gaussian assumption is grossly incorrect for the Heisenberg model, in one dimension, and leads to a qualitatively incorrect spectral function, due to the presence of higher-order cumulant averages that affect significantly the dynamics. The critical exponents were given correctly, however, for the cases considered so far. Preliminary work indicates that this is not so in the ferromagnetic chain, for $q \ll k$, where the mode-coupling theory would predict a finite diffusion constant at $T=0$, and the evidence is that it in fact vanishes as $1/\ln k$, if there is a diffusion process at all. The results for the critical exponents may also be invalid in three dimensions. The susceptibility is proportional to $(q^2 + k^2)^{-2+\eta}$, which is incompatible with the Gaussian assumption (see Appendix A), and does not lead to (B3) from (B1). Whether the mode-coupling prescription is in fact correct to order η remains to be seen. The demonstration that the exponents are correct to first order in an ϵ expansion does not speak to this issue, since η is of order ϵ^2.

---

*This work was begun at the Institute of Theoretical Physics, Chalmers Techniska Hogskola, Sweden.

[1]G. Reiter, Phys. Rev. B 5, 222 (1972).
[2]J. M. J. Van Leeuwen and J. D. Gunton, Phys. Rev. B 6, 231 (1972).
[3]G. Reiter, Phys. Rev. B 7, 3325 (1973).
[4]L. P. Kadanoff and J. Swift, Phys. Rev. 166, 89 (1968).
[5]K. Kawasaki, in *Critical Phenomena*, edited by C. Domb and M. Green (Academic, New York, 1976), Vol. 5A.
[6]F. Wegner, Z. Phys. 216, 433 (1968); 218, 260 (1969).
[7]K. Kawasaki, Prog. Theor. Phys. 37, 285 (1968).
[8]P. Resibois and M. DeLeneer, Phys. Rev. 152, 305 (1966); 152, 318 (1966); 178, 806 (1969); 178, 819 (1969).
[9]M. Blume and J. Hubbard, Phys. Rev. B 1, 3815 (1970).
[10]G. F. Reiter and A. Sjolander, Phys. Rev. Lett. 39, 1047 (1977).
[11]P. Martin, E. Siggia, and H. Rose, Phys. Rev. B 8, 423 (1973).
[12]E. Riedel (private communication).
[13]G. Reiter and F. C. Barreto, Phys. Rev. B 9, 46 (1974).
[14]A. Tucciarone, J. M. Hastings, and L. M. Corliss, Phys. Rev. Lett. 26, 257 (1971); A. Tucciarone, H. Y. Lau, L. M. Corliss, A. Delapalme, and J. M. Hastings, Phys. Rev. B 4, 3206 (1971).
[15]P. Resibois (private communication).
[16]R. H. Kraichnan, in *Statistical Mechanics*, edited by S. A. Rice, K. F. Freed, and J. C. Light (University of Chicago, Chicago, 1972).
[17]D. Dubois, Bull. Am. Phys. Soc. 22, 1149 (1977).
[18]See, however, B. Halperin and P. Hohenberg [Rev. Mod. Phys. (to be published)] for a discussion of the reasons for the small corrections due to the next term in the expansion in the case of the fluids.
[19]R.H. Kraichnan, J. Math. Phys. 2, 124 (1961).
[20]P. Fedders, Phys. Rev. B 12, 3933 (1975).